Simulation of grain seed motion in a hybrid dryer with CFD-DEM coupling approach

Petru-Marian Cârlescu [1], Ioan Țenu [1], Marius Băetu[1], Vlad Arsenoaia[1] and Radu Roșca [1]

[1] *University of Life Sciences, 3 Mihail Sadoveanu Alley, Iași, 700490, Romania*

Abstract

A numerical study of gas-solid flow through an innovative hybrid dryer model was performed using the Discrete Element Method (DEM) and Computational Fluid Dynamics (CFD) coupling methods. In this model, the discrete particle phase (maize seed) was described by EDEM software, and the continuous gas phase (warm air) was described by Fluent software. The optimal geometry of the hybrid dryer in which the maize seeds move, hot air flow and temperature field uniformity were analyzed, being obtained with the coupled approach of CFD-DEM simulation. The simulation results showed that at a velocity of 20-25 m/s of the maize seeds, the residence time required in order for the seeds to be dried in the dryer was obtained. The truncated cone geometry of the hybrid dryer, with a reduced section at the dry seed discharge end and its 5° inclination of the longitudinal axis in the direction of discharge, cause the seeds to move in a circular path in the first half of the dryer and then to be deposited at the lower part of the second half. For low transport velocities in the dryer, the seeds move slowly and concentrated at the end of the hybrid dryer, being periodically unloaded every 3-4 seconds into the collecting cyclone. This DEM-CFD coupling approach is reliable as a tool for understanding the physical phenomenon of seed movement in the airflow field. Numerical simulation of seed movement based on the DEM-CFD coupling approach can provide a theoretical basis for increasing the drying efficiency of maize seeds in the hybrid dryer.

Keywords

hybrid dryer, seed motion, CFD-DEM coupling

1. Introduction

Drying is the most widely used method for preserving maize seeds. In the process of drying the seeds, moisture is removed with high energy and time consumption [1, 2]. The development of technology and software has made it possible to design and simulate new dryer models [3, 4]. Computational Fluid Dynamics (CFD) is a software for simulating fluid flows and describing the characteristics of the flow field and revealing the fluid phase mechanism [5]. The discrete element method (DEM) is applied to study the flow of particles by obtaining dynamic information about the trajectories of particles, the transient forces acting on individual particles. Gas flow and particle motion behavior were studied numerically through CFD-DEM coupling [6, 7, 8, 9, 10]. The coupled CFD-DEM model was adopted to simulate the characteristics of gas-solid flow in fibrous media exposed to particulate loading [11] and to charged particle fluxes in a rotational flow [12]. Particle motion and gaseous flow field for a lime shaft furnace using coupled three-dimensional DEM-CFD were also investigated [13]. In addition, the DEM-CFD coupling approach has been used in many studies to study the mechanism of particle dispersion in gas-solid flux [14, 15, 16, 17, 18, 19, 20, 21]. They found that the simulation results based on the coupled DEM approach with CFD could well explain the mechanism of motion of the fluid and particles that were consistent with the experimental data. CFD-DEM coupled simulation from this paper has the advantage of testing the airflow and particle trajectory inside a drying

Proceedings of HAICTA 2022, September 22–25, 2022, Athens, Greece
EMAIL: pcarlescu@uaiasi.ro (A. 1); itenu@uaiasi.ro (A. 2); rrosca@uaiasi.ro (A. 3)
ORCID: 0000-0003-1039-0412 (A. 1); 0000-0001-5633-522X (A. 2); 0000-0003-4222-2165 (A. 3)

equipment before introducing agricultural seeds into it, helping to optimally design it. Determining the optimal seed entry velocity into the dryer is important to ensure the optimal drying time of the seeds in the dryer.

2. Structure and working principle of hybrid dryer

The structure of the hybrid drying plant was shown as in Figure 1.

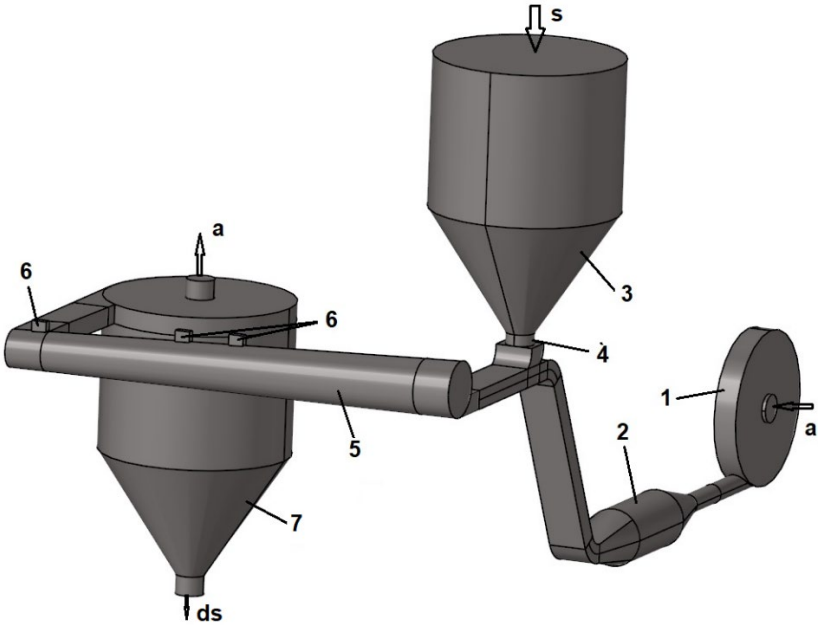

Figure 1: Hybrid dryer (*1* fan; *2* electric heating element; *3* seed bin feed; *4* lock; *5* truncated cone dryer; *6* waveguides with magnetrons; *7* cyclone; *a* air; *s* wet seeds; *ds* dried seeds)

The hybrid dryer model is based on the pneumatic transport of seeds in a stream of air at a temperature of 35-45 °C. In order to keep the seeds inside the dryer long enough so that the microwave heats the maize, a dryer with a truncated cone geometry was designed. Through this geometry of the dryer and the tangential supply of the heterogeneous mixture of seeds-hot air in the interior space, a vortex is formed with certain ratios of its geometric parameters. Thus, the transport route of the seeds through the dryer increases substantially, and the rotation of the seeds helps to standardize the volumetric heating with microwaves. The dimensions of the hybrid drying plant used in the simulation were presented according to Table 1.

Table 1

Dimensions of the hybrid drying plant

Elements	Units (m)
Dryer length	2.5
Large diameter dryer	0.45
Small diameter dryer	0.30
Inlet diameter -warm air	0.20
Inlet diameter -wet seeds	0.15
Inlet size -air seeds mixture	0.2x0.1
Outlet size - air seeds mixture	0.2x0.1
Cyclone diameter	1

2.1. CFD-DEM coupled simulation

The transport of maize seeds inside the dryer is done pneumatically, but the trajectory of the seeds is difficult to follow during operation. CFD-DEM coupled simulation was used to optimize the design of the dryer. The simulation is useful because it allows wide variations of the operating parameters by varying the air flow and the temperature of its entry into the dryer.

2.1.1. Mathematical models of gas-solid

Gas phase model

The simulation of the hybrid dryer by CFD is based on the RNG k-ε turbulence model of the gas phase flow (warm air). This RNG k-ε turbulence model with the dominant vortex flow option is similar in shape to the standard k-ε model, including a number of enhancements [22]. All of these features make this model more accurate and reliable for a wider flow class than the standard model. The gas phase which was treated as continuous phase strictly follows the mass conservation law and momentum conservation laws [6]. The governing equations of mass and momentum conservation in an incompressible viscous fluid could be expressed as:

$$\frac{\partial(\varepsilon_g \rho_g)}{\partial t} + \nabla \cdot (\varepsilon_g \rho_g \overrightarrow{v_g}) = 0, \tag{1}$$

$$\frac{\partial(\varepsilon_g \rho_g \overrightarrow{v_g})}{\partial t} + \nabla \cdot \left(\varepsilon_g \rho_g \overrightarrow{v_g} \otimes \overrightarrow{v_g}\right) = -\varepsilon_g \nabla P + \varepsilon_g \nabla \cdot \tau + \varepsilon_g \rho_g \vec{g} - R_{gp}, \tag{2}$$

where ρ_g , v_g , ε_g, P and τ were air density, air velocity, volume fraction, pressure and viscous stress tensor, respectively. R_{gp} was the momentum exchange between solid and gas phases due to forces exerted by airflow on all particles within the computational cell.

The R_{gp} component was defined as:

$$R_{gp} = \sum_{i=1}^{n} \overrightarrow{F_{p,i}} / \Delta V, \tag{3}$$

where $F_{p,i}$ was the resultant force exerted on particle i, n was the number of particles in the specific computational cell and ΔV was the volume of the cell.

Particle motion equations

The gas phase was considered as an incompressible fluid based on Eulerian-Langrangian approach as the seeds occupied a small space in the hybrid dryer. The seeds were treated as a collection of individual particles whose movement was governed by applying Newton's second law.

The continuum gas phase and dispersed solid phase were coupled in hybrid drier. The particle phase motion was modeled using the Lagrangian approach in which seeds were followed along their trajectories through the unsteady, non-uniform airflow field. The forces of drag, gravity and buoyancy, Saffman lift force and Magnus lift force were taken into account to act on particle. The motion of a particle within airflow field was governed by the force balance equation:

$$m_p \frac{\partial \overrightarrow{v_p}}{\partial t} = \overrightarrow{F_D} + \overrightarrow{F_{GB}} + \overrightarrow{F_{Sa}} + \overrightarrow{F_{Ma}}, \tag{4}$$

$$I_p \frac{d\overrightarrow{\omega_p}}{dt} = \vec{T}, \tag{5}$$

where F_D is the drag force, F_{GB} is the force due to gravity and buoyancy, F_{Sa} is the Saffman lift force, F_{Ma} is the Magnus lift force due to particle rotation, I_p is the moment of the inertia of the particle, ω_p is the angular velocity, T the local torque on the particle, v_p is particle velocity, m_p is particle mass, t is the time.

2.1.2. CFD-DEM coupling simulation method

In the gas-solid coupling simulation, CFD technique and particle motion were based on the softwares Fluent and EDEM (Engineering discrete element method, DEM Solutions Ltd), respectively.

Figure 2 shows how the Fluent CFD software was coupled with EDEM software.

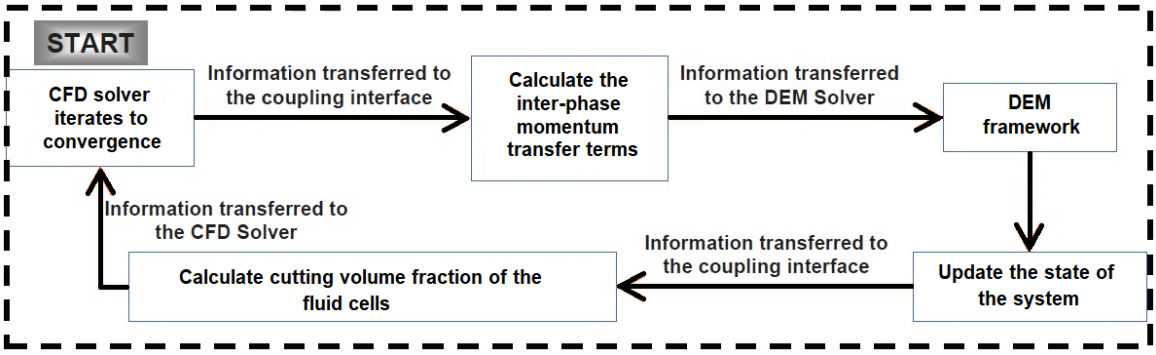

Figure 2: CFD-DEM coupling simulation

In Fluent simulation, all the differential governing equations were solved by applying the finite volumes method and were based on the mass and momentum of the fluid phase according to the mathematical model. First, the airflow field was resolved by CFD solver. When a stable situation was obtained, the gas field from CFD solver was transferred to CFD-DEM coupling interface which imported computation of forces acting on each particle. Then, the EDEM time step started at the end of fluid simulation time step. The calculated interface forces were delivered to the EDEM solver which computed the particle position, particle velocities and particle volume fraction until the end of CFD time step was reached. Next, CFD-DEM coupling interface took the particle translational and rotational motion data from the EDEM solver and computed the volume fractions and momentum exchange in the mesh cell of CFD. Finally, CFD solver used these data to solve the gas field for updating the fluid flow domain. The CFD and EDEM solvers entered into the cycles of the next time step until the airflow field again converged to a stable solution.

The time step Δt in the coupled simulation was chosen small enough to prevent excessive overlaps leading to forces of unrealistic values in practice. The correct time step for DEM simulation is in the range of 10^{-4} to 10^{-6} s, being 10 to 100 times shorter than the time step most often used in CFD simulation. The particles introduced in the simulation were the maize seeds, which were modeled as an assembly consisting of 5 spheres, shown in Figure 3.

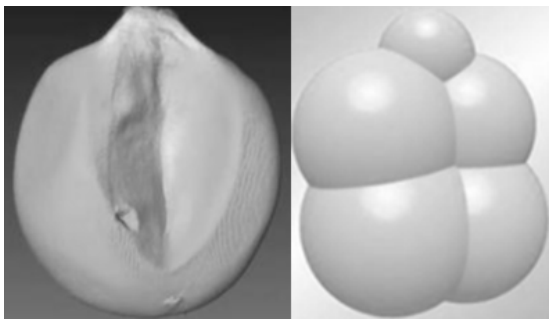

Figure 3: Maize seed modeling in DEM

Computational conditions and parameters

The CFD-DEM coupled simulation starts from the 3D geometry of the drying plant. The fan has been removed from the installation for simplification. The discretization grid with tetrahedral cells in the drying plant was made with the Gambit software. A study of the independence of the grid with three different densities of discretization was carried out, with a number ranging from 27,120,000; 4,312,000 to 2,350,000 volumes. A discretization density of 4,312,000 volumes was found to be optimal for simulation resulting in a reasonable computation time (Figure 4). The Lagrangian coupling method was used in the EDEM-CFD coupling interface. The 5-sphere hard model and the Hertz-Mindlin (non-slip) model were chosen as the particle model and particle contact model in the EDEM software for maize seed.

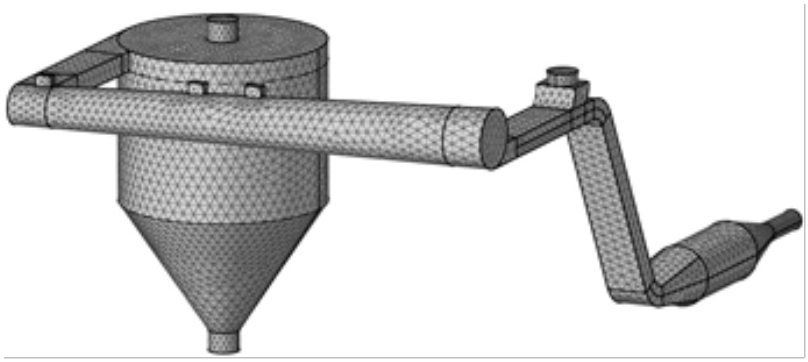

Figure 4: Schematics of computational grids

The values of main parameters used in the DEM-CFD coupling simulations are listed in Table 2.

Table 2

Computational parameters used in the simulations

Contact type (phase)	Parameter	Value for maize seed	Value for steel
	Particle type	5 spheres	
	Semi-axes (mm x mm x mm)	4.5x8.9x10.8	
	Density (kg/m^3)	661	7800
	Poisson's ratio	0.4	0.3
	Shear modulus (Pa)	2.48x10^7	7.93x10^{10}
Seed to seed (solid)	Coefficient of restitution	0.254	
	Coefficient of static friction	0.5	
	Coefficient of rolling friction	0.01	
Seed to steel wall (solid)	Coefficient of restitution	0.612	
	Coefficient of static friction	0.165	
	Coefficient of rolling friction	0.01	
	Solid time step (s)	5x10^{-6}	
Gas phase (fluid)	Gravitational acceleration (m/s^2)	9.81	
	Density (kg/m^3)	1.225	
	Viscosity (kg/m/s)	1.7894x10^{-5}	
	Fluid time step (s)	1x10^{-3}	

The velocity of the warm air at the entrance to the mixing zone was chosen so as to ensure the pneumatic transport of maize seeds at 20-25 m/s at an average temperature of 48 ºC, and the flow rate of seeds entering the drying plant was 500 kg/h.

3. Results and discussion

The results of the warm air flow obtained by simulating the CFD in the hybrid dryer are presented by the velocity, temperature and pathlines. The distribution of the velocity and temperature gradients obtained on the section of the truncated cone dryer are shown according to Figure 5 and Figure 6. In the center of the dryer, on a length of about 1.5 m, the velocity is lower (dark color) and the geometric shape created is approaching a cone. In order to maintain a pneumatic transport velocity of the seeds at the periphery of the dryer, its truncated cone shape was adopted. If cross sections are made on different lengths of the dryer, Figure 7, the distribution of rotational velocity vectors is observed, and the flow velocity decreases from the periphery to the center of the dryer on its axis of symmetry. From these observations, taking into account the distribution of pathlines, it was estimated that inside the dryer the maize seeds rotate in the direction of rotation of the vortex, having a translational movement from the input to output from the dryer Figure 8.

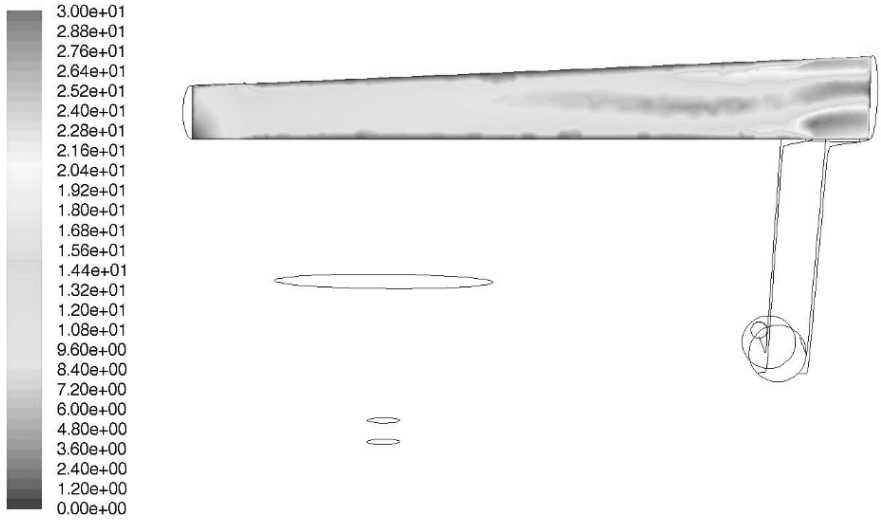

Figure 5: Velocity field distribution in dryer (m/s)

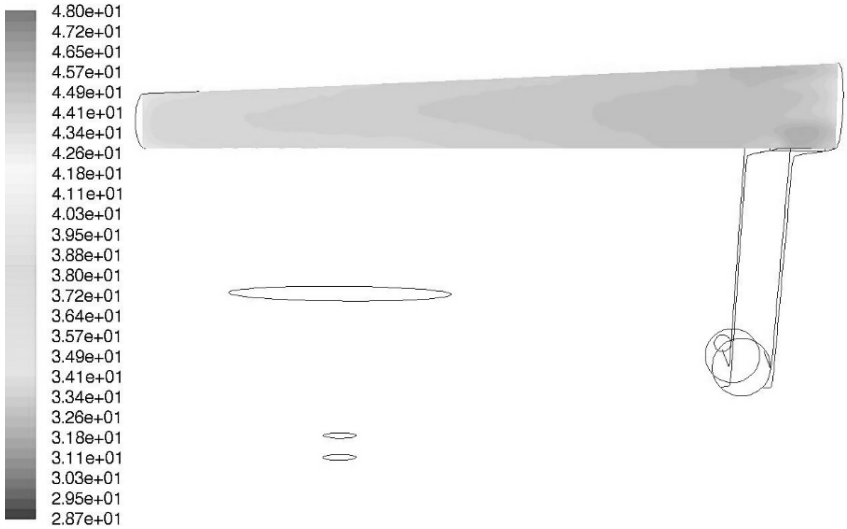

Figure 6: Temperature field distribution in dryer (^{o}C)

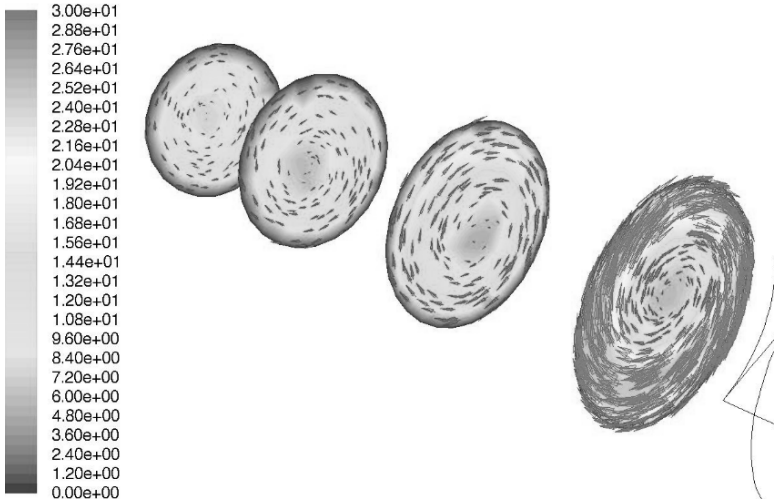

Figure 7: Velocity field and velocity vectors in four sections along the length of the dryer (m/s)

Figures 5 and Figure 7 show a variation of the velocity in the field inside the truncated cone dryer, which is 12-18 m/s near the inner walls of the dryer and between 20 - 25 m/s in the rest, thus ensuring the pneumatic transport of seeds.

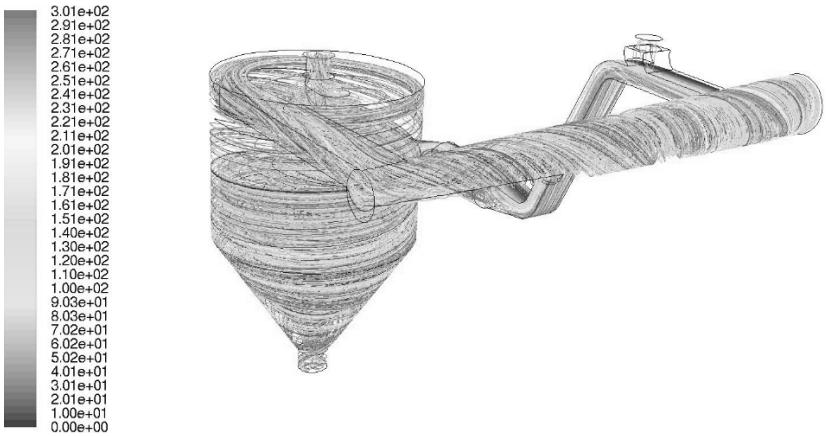

Figure 8: Pathlines in dryer and cyclone (-)

The trajectory of maize seeds observed by DEM simulation is shown in Figure 9.

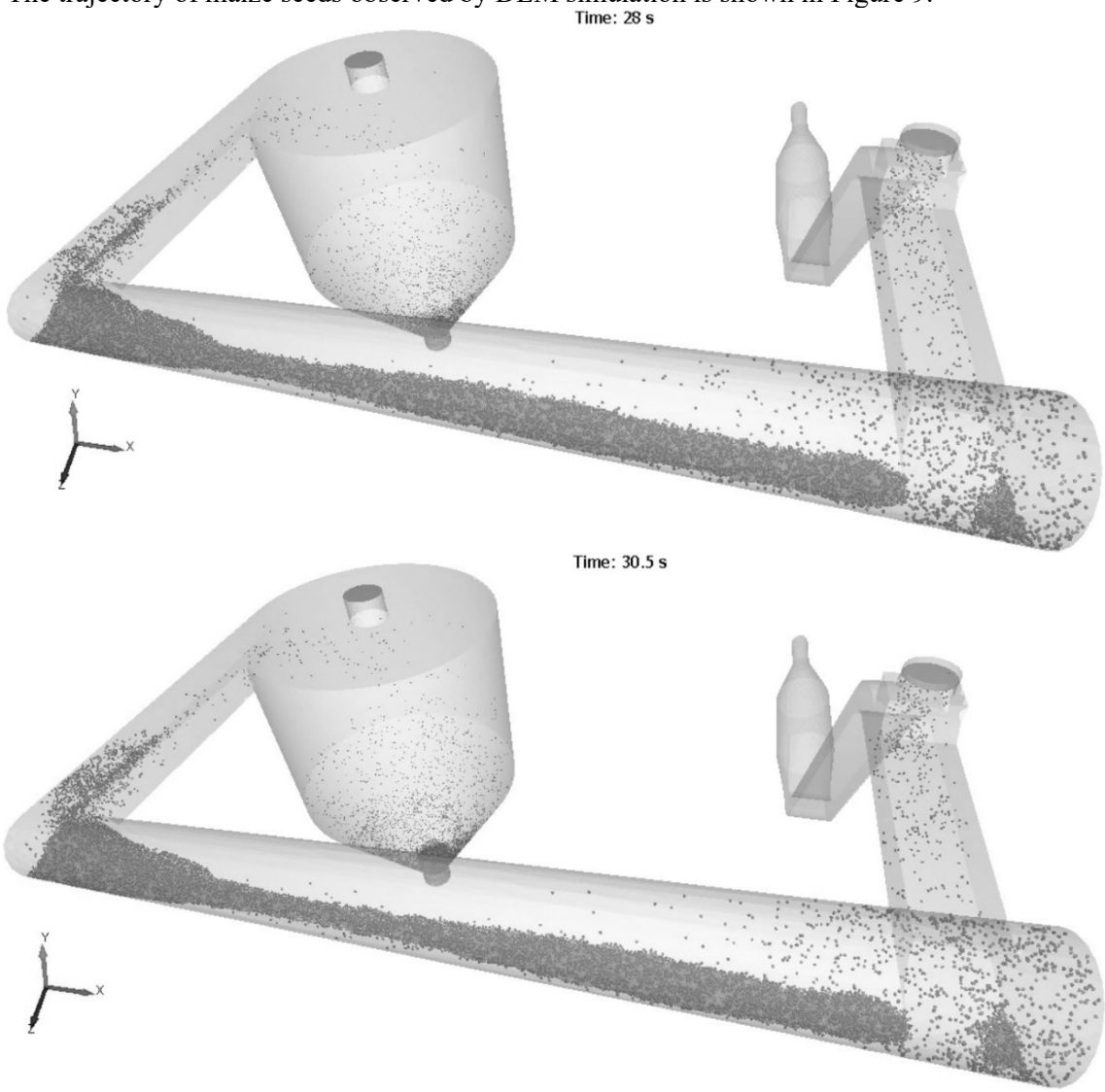

Figure 9: Distribution of maize seeds in dryer and separation cyclone for two periods (28 s; 30.5 s)

Thus, Figure 9 shows the tendency for maize seeds to agglomerate at the bottom of the dryer. Due to the distribution of the velocity vectors in four cross sections along the length of the dryer (Figure 7), the seeds follow the same circular path up to the middle of the dryer when the tangential velocity decreases and the corresponding size of the velocity vectors is smaller. Due to the decrease of the section

towards the outlet end of the truncated cone dryer, the transport velocity is maintained but with vectors in the longitudinal direction, so the seeds deposited at the bottom of the dryer due to gravity in the direction of the axis (-OY) move to the exit and the slight inclination of the dryer at an angle of 5º in the direction of seed discharge. The seeds are moved in a circular motion in the first half of the dryer and then deposited at the bottom of the dryer where they are collected at the end of the drill where they are unloaded in larger quantities periodically every 3-4 seconds, Figure 9. The maize seed passes through the dryer for a maximum of 20 seconds, long enough for the action of the microwave in the volume of the seeds, causing their temperature to rise to 44 °C.

4. Conclusions

In this research, the DEM-CFD coupling approach in the design of the hybrid dryer leads to the following conclusions:

The characteristics of the air flow and the trajectories of the seed lead to a circular motion in the first half of the dryer and a deposition at the bottom in the second half of it.

The optimum design of the hybrid dryer is a truncated cone geometry with a large base in the seed inlet region and a small base in the dry seed outlet region.

The proper airflow inlet velocity and seeds in the dryer is 20 – 25 m/s, which provides the time required for the seeds to stand in the dryer for drying.

Numerical seed motion simulation based on the DEM-CFD coupling approach can improve the performance of the hybrid dryer.

5. Acknowledgements

This work was supported by a grant of the Romanian Ministry of Education and Research, project number CNCS/CCCDI-UEFISCDI, project number PN-III-P2-2.1-PED-2019-3001, within PNCDI III, contract no. 378PED/2020. Thanks for all your support.

6. References

[1] B. Dieter, S. Karl, Heat and mass transfer, Springer-Verlag, Berlin, 2006.

[2] D. Incopera, T. Bergman, Fundamentals of heat and mass transfer, John Wiley and Sons, New York, 2007.

[3] R. P. Ramachandran, M. Akbarzadeh, J. Paliwal, S. Cenkowski, Computational Fluid Dynamics in Drying Process Modelling – a Technical Review, Food and Bioprocess Tehnology (2017) 1-22.doi: 10.1007/s11947-017-2040-y.

[4] T. A. G. Langrish, J. Harrington, X. Huang, C. Zhong, Using CFD Simulation to Guide the Development of a New Spray Dryer Design, Processes 8 (2020) 932 1-22.doi: 10.3390/pr8080932.

[5] H. C. Li, Y. M. Li, F. Gao, Z. Zhao, L. Z. Xu, CFD-DEM simulation of material motion in air-and-screen cleaning device, Comput. Electr. Agri. 88 (2012) 111–119.doi: 10.1016/j.compag.2012.07.006.

[6] S.L. Yang, K. Luo, K. Zhang, K.Z. Qiu, J.R. Fan, Numerical study of a lab-scale double slot-rectangular spouted bed with the parallel CFD-DEM coupling approach, Powder Technol. 272 (2015) 85–99.doi:10.1016/j.powtec.2014.11.035.

[7] Z.B. Peng, B. Moghtaderi, E. Doroodchi, A modified direct method for void fraction calculation in CFD-DEM simulations, Adv. Powder Technol. 27 (2016) 19–32.doi: 10.1016/j.apt.2015.10.021.

[8] S.B. Kuang, K. Li, R.P. Zou, R.H. Pan, A.B. Yu, Application of periodic boundary conditions to CFD-DEM simulation of gas-solid flow in pneumatic conveying, Chem. Eng. Sci. 93 (2013) 214–228.doi:10.1016/j.ces.2013.01.055.

[9] P. Traore, J.C. Laurentie, L. Dascalescu, An efficient 4 way coupling CFD-DEM model for dense gas-solid particulate flows simulations, Comput. Fluids 113 (2015) 65–76. doi: 0.1016/j.compfluid.2014.07.017.

[10] S. Akhshik, M. Behzad, M. Rajabi, CFD-DEM approach to investigate the effect of drill pipe rotation on cuttings transport behavior, J. Petrol. Sci. Eng. 127 (2015) 229–244.doi: 10.1016/j.petrol.2015.01.017.
[11] F.P. Qian, N.J. Huang, J.L. Lu, Y.L. Han, CFD-DEM simulation of the filtration performance for fibrous media based on the mimic structure, Comput. Chem. Eng. 71 (2014) 478–488.doi: 10.1016/j.compchemeng.2014.09.018.
[12] V. Akbarzadeh, A.N. Hrymak, Coupled CFD-DEM of particle-laden flows in a turning flow with a moving wall, Comput. Chem. Eng. 86 (2016) 184–191.doi: 10.1016/j.compchemeng.2015.12.020.
[13] B. Krause, B. Liedmann, J. Wiese, S. Wirtz, V. Scherer, Coupled three dimensional DEM-CFD simulation of a lime shaft kiln-Calcination, particle movement and gas phase flow field, Chem. Eng. Sci. 134 (2015) 834–849.doi: 10.1016/j.ces.2015.06.002.
[14] N. Iqbal, C. Rauh, Coupling of discrete element model (DEM) with computational fluid mechanics (CFD): a validation study, Appl. Math. Comput. 277 (2016) 154–163.doi: 10.1016/j.amc.2015.12.037.
[15] T. Brosh, H. Kalman, A. Levy, I. Peyron, F. Ricard, DEM-CFD simulation of particle comminution in jet-mill, Powder Technol. 257 (2014) 104–112.doi: 10.1016/j.powtec.2014.02.043
[16] H. Zhou, G.Y. Mo, J.P. Zhao, K.F. Cen, DEM-CFD simulation of the particle dispersion in a gas-solid two-phase flow for a fuel-rich/lean burner, Fuel 90 (2011) 1584–1590.doi: 10.1016/j.fuel.2010.10.017.
[17] D.Y. Liu, C.S. Bu, X.P. Chen, Development and test of CFD-DEM model for complex geometry: a coupling algorithm for Fluent and DEM, Comput. Chem. Eng. 58 (2013) 260–268.doi: 10.1016/j.compchemeng.2013.07.006.
[18] X. D. Liu, Y. P. Chen, Y. F. Chen, Analysis of gas-particle flow characteristics in impinging streams, Chem. Eng. Process. 79 (2014) 14–22.doi: 10.1016/j.cep.2014.02.006.
[19] M. L. Liu, Y. Y. Wen, R.Z. Liu, B. Liu, Y. L. Shao, Investigation of fluidization behavior of high density particle in spouted bed using CFD-DEM coupling method, Powder Technol. 280 (2015) 72–82.doi:10.1016/j.powtec.2015.04.042.
[20] Y. Z. Zhao, Y. l. Ding, C. N. Wu, Y. Cheng, Numerical simulation of hydrodynamics in downers using a CFD-DEM coupled approach, Powder Technol. 199 (2010) 2–12.doi: 10.1016/j.powtec.2009.04.014.
[21] L. Xiaolong, L. Yitao, L. Qingxi, Simulation of seed motion in seed feeding device with DEM-CFD coupling approach for rapeseed and wheat, Computers and Electronics in Agriculture 131 (2016) 29-39.doi: 10.1016/j.compag.2016.11.006.
[22] Ansys Inc., Ansys Fluent Theory Guide 20R1, 2020, URL: https://d.shikey.com/down/Ansys.Products.2020.R1.x64/install_docs/Ansys.Products.PDF.Docs.2020R1/readme.html.